

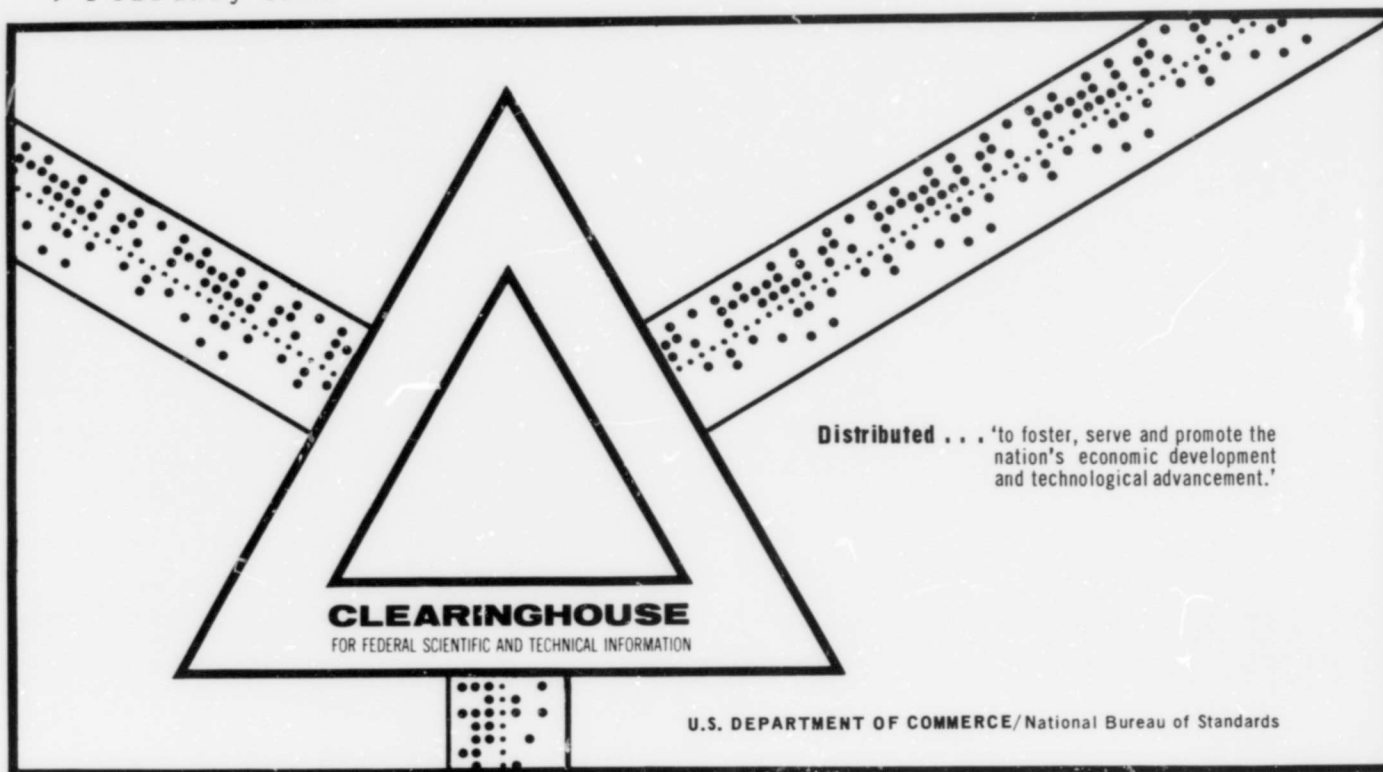
AD 701 377

DETECTION OF TITAN POGO CHARACTERISTICS BY ANALYSIS OF  
RANDOM DATA

R. G. Wagner, et al

Aerospace Corporation  
El Segundo, California

9 February 1970



This document has been approved for public release and sale.

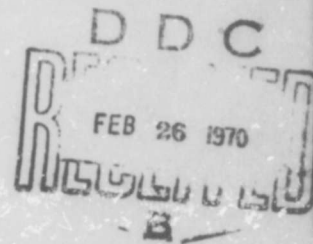
AD701377

## Detection of Titan Pogo Characteristics by Analysis of Random Data

Prepared by R. G. WAGNER and S. RUBIN  
Applied Mechanics Division

70 FEB 09

Engineering Science Operations  
THE AEROSPACE CORPORATION



Prepared for SPACE AND MISSILE SYSTEMS ORGANIZATION  
AIR FORCE SYSTEMS COMMAND  
LOS ANGELES AIR FORCE STATION  
Los Angeles, California

Reproduced by the  
CLEARINGHOUSE  
for Federal Scientific & Technical  
Information Springfield Va. 22151

THIS DOCUMENT HAS BEEN APPROVED FOR PUBLIC  
RELEASE AND SALE; ITS DISTRIBUTION IS UNLIMITED

**BLANK PAGE**

Air Force Report No.  
SAMSO-TR-70-22

Aerospace Report No.  
TR-0066(5305)-3

**DETECTION OF TITAN POGO CHARACTERISTICS BY  
ANALYSIS OF RANDOM DATA**

**Prepared by**

**R. G. Wagner  
and  
S. Rubin**

**Applied Mechanics Division**

**70 FEB 09**

**Engineering Science Operations  
THE AEROSPACE CORPORATION  
El Segundo, California**

**Prepared for**

**SPACE AND MISSILE SYSTEMS ORGANIZATION  
AIR FORCE SYSTEMS COMMAND  
LOS ANGELES AIR FORCE STATION  
Los Angeles, California**

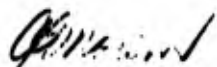
**This document has been approved for public  
release and sale; its distribution is unlimited**

## FOREWORD

This report is published by The Aerospace Corporation, El Segundo, California under Air Force Contract F04701-69-C-0066. Research is documented which was carried out from August 1963 through July 1969.

The report was submitted on 20 November 1969 to James P. Cooper, Lt. Col., USAF, for review and approval.

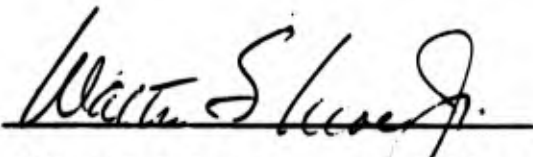
Approved



---

A. G. Norem, Director  
Systems Evaluation Subdivision  
Applied Mechanics Division

Publication of this report does not constitute Air Force approval of the report's findings or conclusions. It is published only for the exchange and stimulation of ideas.



---

WALTER S. MOE, JR., Colonel, USAF  
Deputy Director for Engineering & Test  
The MIB System Program Office

## ABSTRACT

Dynamic characteristics of Titan vehicles related to the Pogo phenomenon have been found through the analysis of low-level random accelerations and pressures from ground test and flight data. Natural frequencies of vibration of propellant suction lines and of flight vehicle longitudinal motion have been successfully detected from locations of peaks in auto spectra. The inflight performance of a standpipe accumulator has been evaluated by means of both auto-spectral and cross-spectral analyses. An anomalous occurrence of Pogo vibration on one flight was explained by the analysis as due to a lack of normal gas charge in the standpipes. A novel method is applied to the evaluation of the longitudinal structural dynamic model of the vehicle. The method involves the detection of "node frequencies" at locations of accelerometers. By this method specific modeling deficiencies were identified and corrected for a Titan vehicle configuration, thereby greatly improving the correlation of flight-derived and analytical natural frequencies.

## SYMBOLS

B	bandwidth (Hz)
$G_x(f)$	auto-spectral density of $x(t)$
$G_{xy}(f)$	cross-spectral density of $x(t)$ and $y(t)$
$H(f)$	frequency-response function
T	duration of data (sec)
f	frequency (Hz)
n	number of statistical degrees of freedom
p	pressure
t	time
$x(t), y(t)$	functions of time
$\ddot{x}$	acceleration
$\gamma^2(f)$	coherence function

## CONTENTS

ABSTRACT . . . . .	iii
SYMBOLS . . . . .	iv
I. INTRODUCTION . . . . .	1
II. NATURE OF THE DATA AND DATA REDUCTION . . . . .	5
III. DETECTION OF RESONANT FREQUENCIES . . . . .	9
A. Engine Static Firings . . . . .	9
B. Vehicle Flights . . . . .	14
IV. EVALUATION OF A STANDPIPE ACCUMULATOR . . . . .	21
V. EVALUATION OF THE LONGITUDINAL STRUCTURAL DYNAMIC MODEL . . . . .	31
A. Detection of Modeling Deficiencies. . . . .	34
VI. SUMMARY AND CONCLUSIONS . . . . .	41
REFERENCES . . . . .	45

## FIGURES

1.	Pogo Phenomenon . . . . .	2
2.	Schematic of "Engine Transfer Function Test" Configuration . . . . .	10
3.	Auto-Spectra of Fuel and Oxidizer Suction Pressures . . . . .	12
4.	Schematics of Pogo Accumulators on Gemini Launch Vehicle . . . . .	16
5.	Analytical Versus Flight-Observed Modal Frequencies . . . . .	17
6.	Auto-Spectrum of Flight Acceleration Data . . . . .	18
7.	Effect of Standpipe on Suction Pressure per Unit Pump Acceleration . . . . .	22
8.	Auto Spectrum of Oxidizer Suction Pressure with Standpipe From GT-4 at 60 Percent Stage I Burn Time . . . . .	24
9.	Frequency Response $p_s/p_g$ and Coherence Function from GT-4 Flight at 97 Percent Burn Time . . . . .	25
10.	Frequency Response $p_s/p_g$ from GT-4 and GT-5 Flights at 2.5 Percent Stage I Burn Time . . . . .	27
11.	Auto Spectra of Oxidizer Suction Pressure $p_{sO}$ for Several Flights . . . . .	28
12.	Basics for "Node-Frequency" Detection . . . . .	32
13.	A Titan Vehicle Configuration . . . . .	35
14.	Acceleration Amplitude Ratios Versus Frequency . . . . .	37
15.	Analytical Versus Flight Observed Modal Frequencies, Stage II Burn . . . . .	39

## I. INTRODUCTION

The interpretation of spectral analyses of random data has been of great value in efforts to suppress longitudinal instability (Pogo) on Titan vehicles. The data employed are the low-level random responses of the vehicle structural and propulsion systems during flight, and similar responses of the propulsion system during static firings of engines. The purpose of this report is to describe the manner in which certain vital information concerning the dynamic characteristics of the systems has been extracted from this system "noise." Hopefully, the successes described here will provide ideas and encouragement for other applications.

The now "classical" Pogo instability (Refs. 1-4) results in the spontaneous development of vehicle longitudinal vibration. It has occurred on Thor, Titan and Saturn launch vehicles -- all within the frequency range of 5 to 30 Hz. Changing conditions during the launch cause a period of structural/propulsion system instability to arise. Primarily, the vibrations have occurred in the first longitudinal structural mode during boost of the first liquid stage. This mode has a simple accordion-like behavior in which the two ends of the vehicle vibrate in anti-phase.

The Pogo instability phenomenon results from the regeneration of vehicle longitudinal vibration through the dynamic response of the propulsion system as indicated in Figs. 1a and 1b. An instability occurs when a small longitudinal acceleration ( $\ddot{x}$ ) causes forces to be generated by the propulsion system which then cause intensification of the original vibration. When the system becomes unstable, vibration in the unstable mode of the system grows in amplitude until nonlinear behavior comes into play to stop further growth.

The dominant characteristics of the analytical model for the Pogo phenomenon are: (1) the longitudinal natural vibration modes of the over-all vehicle (for example, the modal frequencies  $f_A$  and  $f_B$  in Fig. 1c), (2) the vibration modes of the propellant columns in the suction lines from tanks to

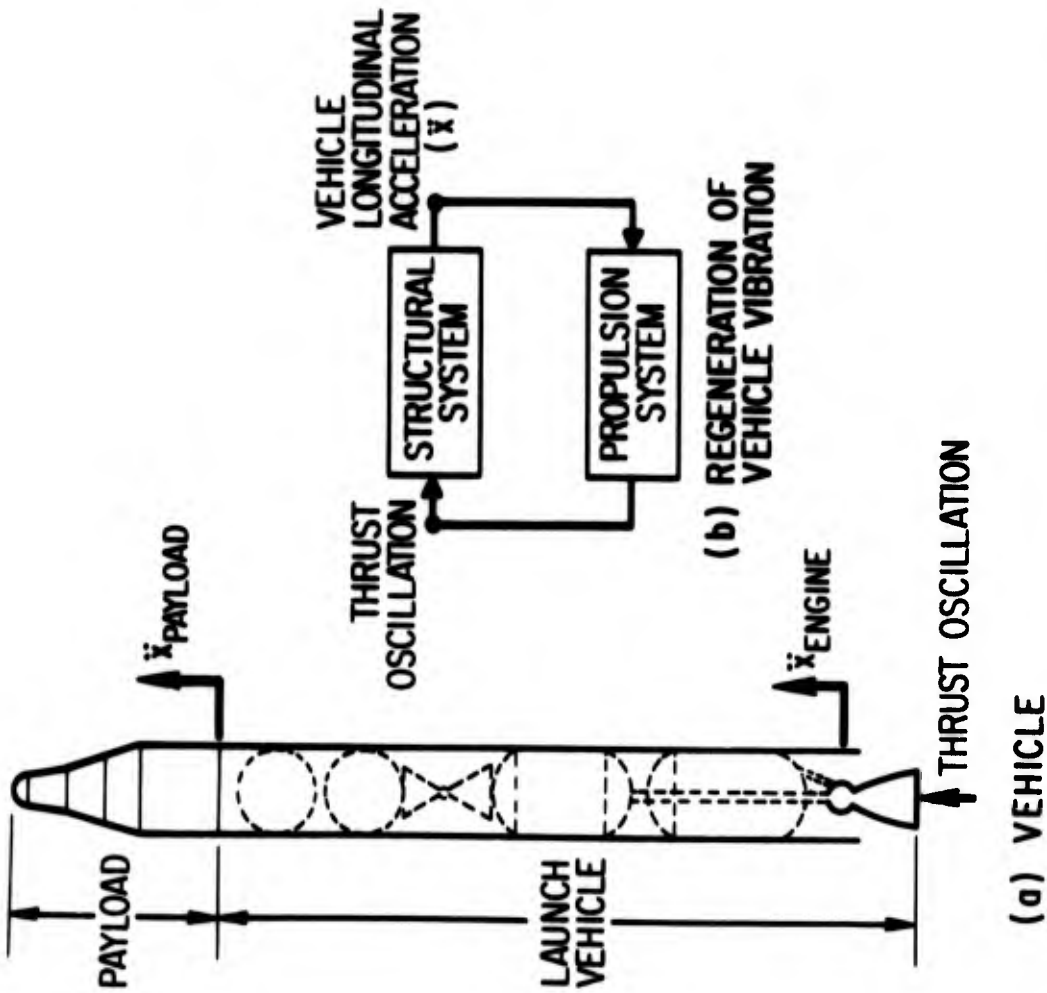
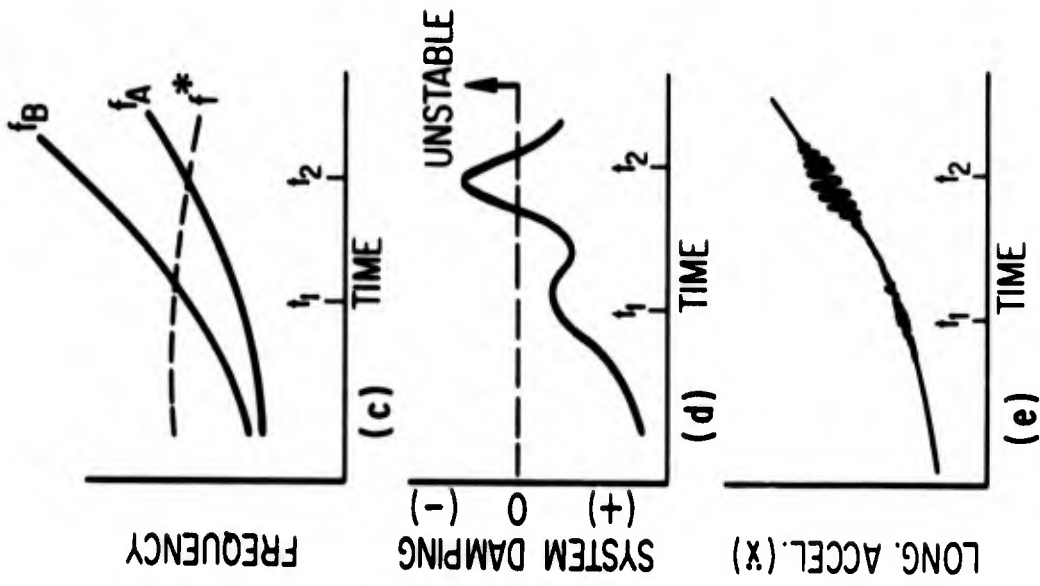


Fig. 1. Pogo Phenomenon

engines, including the effect of local compliance at the pump inlet due to cavitation (for example,  $f^*$  in Fig. 1c), and (3) the frequency response of the engine proper (largely resistive and inertial hydraulic properties). The vibration modes of the vehicle and suction lines vary with time of flight, largely due to propellant depletion and changes in pump operating conditions, respectively. The tendency toward instability (as indicated by the system damping plot in Fig. 1d) increases with reduced separation of the frequency of a structural mode and a suction line mode. In Fig. 1e we depict the system vibration corresponding to the system damping in Fig. 1d. At a time such as  $t_1$  when the system damping is positive, but quite small, the random vibrations of the system are expected to intensify because of increased responsiveness of the system. At  $t_2$  the system is unstable and slowly-varying sinusoidal vibration builds up and then decays as the system passes through the unstable regime. The method that has proven to be practical and effective for stabilizing the system employs hydraulic accumulators to shift the suction line resonant frequencies away from those of critical vehicle modes.

Clearly, much can be learned about the system from data acquired during an instability. The mere fact that the system becomes unstable in the observed time period is vital information. In addition, the interrelationship of the oscillation of the system variables (accelerations, pressures, ...) is a display of the "mode shape" of the unstable mode. These facts provide means for assessing the quality of an analytical model for the system stability; yet, this information is limited since the strong oscillations during an instability effectively mask response information at other frequencies. Moreover, an instability exists only over a small interval of flight. Thus the observation of an instability provides only a glimpse at the character of one mode of the coupled system.

On the other hand, random vibrations of a stable system are not usually overwhelmingly dominated by one mode of the system, and they exist over most or all of the flight duration. These vibrations represent the flight system response to broad-band excitations from sources such as aerodynamic,

propellant pumping and flow, and combustion processes. The system responds by filtering this excitation through its own frequency-dependent characteristics. The hope is that these characteristics can be extracted from the random response data.

The objectives of the analysis of random data for the Pogo problem on Titan vehicles are to

1. Detect system dynamic characteristics
2. Employ such detected characteristics to verify or upgrade analytical models of the structural and propulsion systems
3. Monitor the performance of accumulator devices during vehicle flight
4. Establish norms for flight data as an aid to detection and interpretation of anomalous behavior

Useful information has been obtained through auto-spectral and cross-spectral density analyses of accelerometer and pressure signals from ground firings of engines and from vehicle flights. After discussing the data and its reduction in general terms, we cover the following selected experiences: (1) the detection of resonant frequencies of the vehicle and of the suction lines, (2) the evaluation of a standpipe accumulator, and (3) a novel method for evaluation of the longitudinal dynamic model of the structure.

## II. NATURE OF THE DATA AND DATA REDUCTION

Most flight data were obtained in digital form via a PCM (Pulsed Code Modulated) telemetry system. The sampling rates were either 200 or 400 per second, and the digitizing amplitude interval was 0.4 percent of full range. Some of the flight acceleration data were obtained in continuous form via FM-FM telemetry; all ground test data were continuous. The continuous data were digitized at the 200 or 400 rates for analysis. In most cases the random data were at a low level, with the rms value less than three percent of the full measurement range. Surprisingly, some useful information was obtained for narrow-band data where the rms value was on the same order as the size of the digital amplitude interval. In some instances, narrow-range (in the amplitude sense) measurements were made specifically to improve the detection of the low-level data.

The data reduction consisted of digital auto-spectral\* and cross-spectral density analyses (Ref. 5). Useful information was found in the frequency range up to 30 Hz. Short time spans for the analyses were chosen to minimize effects of nonstationarity associated with changing resonances of the system. In addition, narrow analysis bandwidths were employed to allow resolution of closely-spaced system frequencies. Most analyses were performed with an effective bandwidth (B) of 1 Hz over 4-second time intervals (T). Although these imply eight statistical degrees of freedom n, where

$$n = 2BT \quad (1)$$

bandwidths of narrow-band peaks in the data were in some cases less than the analysis bandwidth; the associated degrees of freedom in the analysis were therefore actually lower than eight. Acceleration data, for example, contained narrow-band spectral peaks with bandwidths of less than 0.5 Hz (based on the expected low damping of the structure of the order of one percent of critical).

---

\*The term "auto-spectral density" is used instead of "power spectral density."

Ordinarily, the number of degrees of freedom is an indicator of the statistical accuracy of the analysis; the higher the better. However, this indicator is not overly important for the particular applications of the analyses employed here. Specific support for this statement is provided below. The ultimate justification lies in the success achieved in extracting results of engineering significance.

One use of the data is the detection of center frequencies of narrow-band energy concentrations corresponding to system resonant frequencies. The accuracy of such detection is more a function of the number of zero crossings within the analysis time than of the bandwidth-time product.

A second use of the data is the estimation of a frequency-response function  $H(f)$  from two random signals. We assume that one signal  $y(t)$  is a response of a linear, constant-parameter system -- and that the second signal  $x(t)$  is the only input. The function  $H(f)$  then describes the amplitude and phase relationship of  $y(t)$  to  $x(t)$  under sinusoidal conditions at the frequency  $f$ . When the two signals are random, the following relationships hold (Ref. 5):

$$H(f) = G_{xy}(f)/G_x(f); \quad |H(f)|^2 = G_y(f)/G_x(f) \quad (2)$$

where  $G_x(f)$  and  $G_y(f)$  are the auto-spectral densities of  $x$  and  $y$ , respectively, and  $G_{xy}(f)$  is the cross-spectral density of  $x$  and  $y$ .

In practice, a number of factors can detract from the statistical accuracy of the results of Eq. (2). Examples of such factors are a lack of linearity, the presence of extraneous noise, and the presence of multiple inputs. (See Ref. 5 for a fuller discussion.) As a result of these factors the two signals are not totally correlated (that is, not completely coherent). The coherence function  $\gamma^2(f)$  is a measure of the degree of correlation at the frequency  $f$ .

Total correlation implies  $\gamma^2 = 1$  and no correlation implies  $\gamma^2 = 0$ . By definition

$$\gamma^2(f) = \frac{|G_{xy}(f)|^2}{G_x(f) G_y(f)} \quad (0 \leq \gamma^2 \leq 1) \quad (3)$$

Thus, in addition to the number of degrees of freedom, statistical accuracy in estimating frequency-response functions depends also on the coherence function. In the examples to be presented, the high coherence (typically above 0.95) apparently counteracts the effect of low degrees of freedom sufficiently well that good engineering results in the estimation of frequency-response information are obtained.

**BLANK PAGE**

### III. DETECTION OF RESONANT FREQUENCIES

#### A. ENGINE STATIC FIRINGS

Special engine static firings have been conducted with the Titan Stage I engine for the Pogo problem. A series of tests called the "Engine Transfer Function Tests" was performed primarily to detect the dynamic characteristics of the engine and suction lines (Ref. 6). The test configuration is shown schematically in Fig. 2. Only one of two engines was present for the test. The oxidizer and fuel suction lines (tank to pump lines) are representative of the flight configuration, except for branch sections near the pump inlets. Sinusoidal piston motion within these branches introduced flow perturbations, thereby allowing frequency-response information to be determined.

A main objective was to investigate a hypothesis that cavitation at a pump inlet was substantially reducing the first resonant frequency of the suction line. Pulsing at discrete frequencies was performed in the range of 6 to 19 Hz at several amplitude levels and for several operating points of the pumps. The pulsing tests showed that the engine responds in a resonant fashion due to excitation of either the oxidizer or fuel circuits. The fundamental engine resonances are due to resonance of the propellant columns in the suction lines. Further, it was found that pump-induced cavitation can reduce the fundamental suction line resonant frequency by more than a factor of two for the 28-foot oxidizer line and by an order of magnitude for the 3-foot fuel line. Without cavitation, the first suction line resonances would be quarter-wave resonances for the distributed properties of the lines (15 Hz for the oxidizer line and above 100 Hz for the fuel line).

For the purposes of this report, the primary data of interest were collected during the periods of pulser inaction. Such data were subjected to auto-spectral density analysis to determine if suction line resonances could be detected from self-induced random excitation of the operating engine. The reference for this evaluation was the forced response determinations.

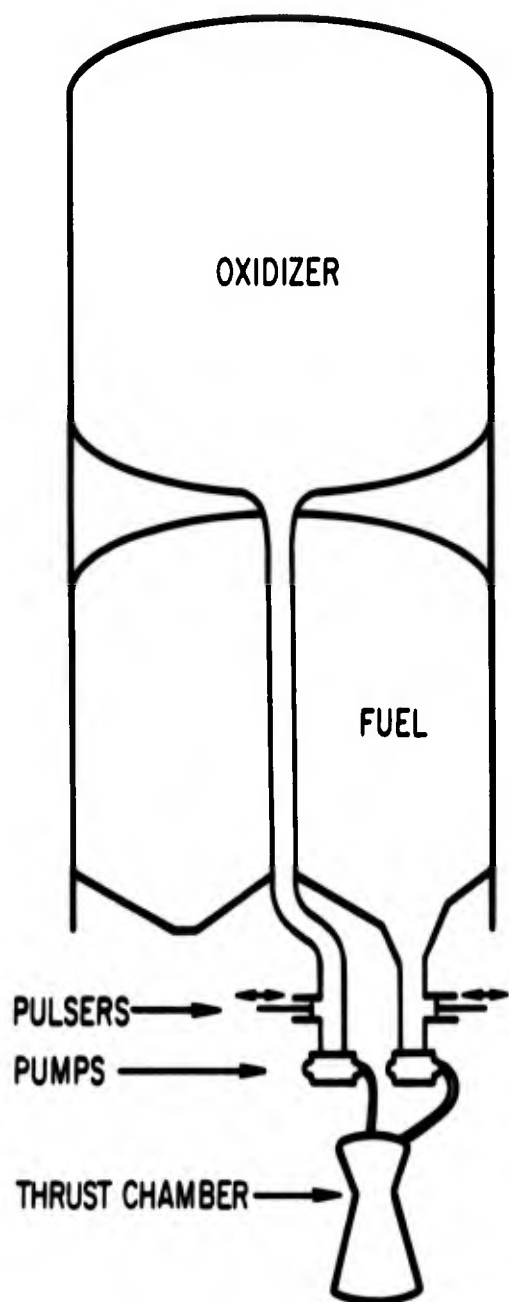


Fig. 2. Schematic of "Engine Transfer Function Test" Configuration

It was recognized that the task would be complicated by several factors. First, the oxidizer resonance is heavily damped (0.2 to 0.3 fraction of critical). Difficulty in distinguishing a peak in the spectra was therefore anticipated. The fraction of critical damping for the fuel resonance is 0.05 to 0.1, so less difficulty was anticipated. A second complication was the presence of the first vertical structural resonance of the test stand within the frequency range of interest. This resonance might obscure or be confused with a suction line resonance. Thirdly, the level of self-induced oscillation was quite low relative to the ranges of the instruments; therefore, instrumentation system noise might overpower the random engine response data. Finally, the observed resonances of the suction lines are affected by dynamic interaction with the hydraulics of the engine proper and perhaps with structural motion. The effect of such coupling may have to be removed to permit accurate interpretation of the results.

One particular period in the second test of the series was unique in that a large excursion of mean fuel inlet pressure was traversed, leading to a varying suction line frequency. Because of the continual rate of change of this pressure, auto-spectral analyses were carried out for two-second samples. Thus, lack of stationarity of the data would not result in excessive smearing of the fuel resonant peaks.

The result for a selected pair of fuel and oxidizer suction pressures is shown in Fig. 3. Armed with the location of the test stand structural resonance (easily seen on acceleration data) and spectra for a wide range of pump operating conditions, the fuel resonant frequency can be identified clearly on Fig. 3. The fuel resonance stands out on both the fuel and oxidizer pressures (and other engine pressures). The presence of the fuel resonant frequency in the oxidizer suction pressure results from coupling through the thrust chamber. The rms value of fuel pressure is only about 4-1/2 percent of full range; even so, the signal/noise ratio is quite acceptable.

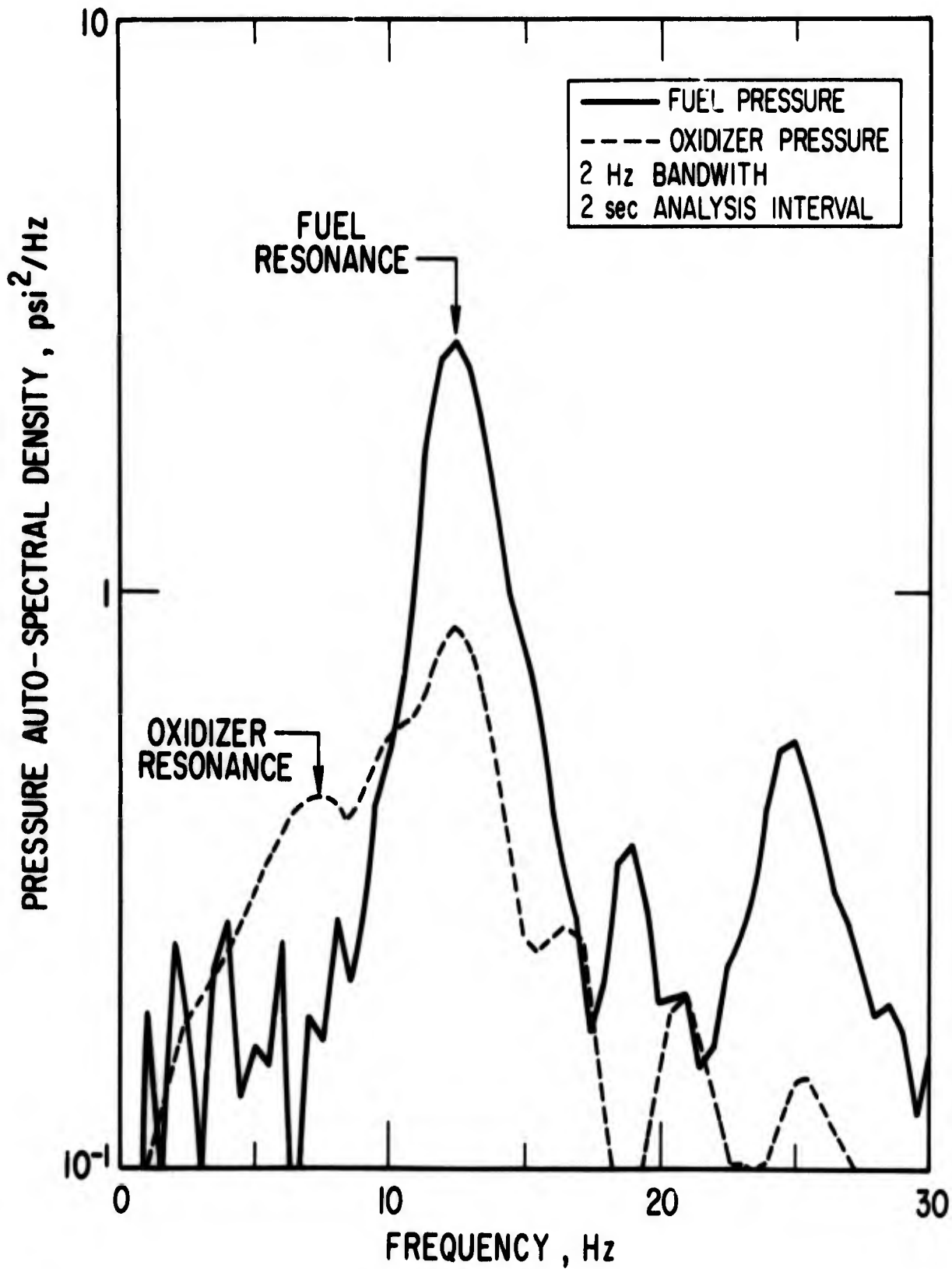


Fig. 3. Auto-Spectra of Fuel and Oxidizer Suction Pressures

The fuel frequency was successfully identified over a wide range of mean pressures by this method. The results were consistent with those determined from the forced response of the engine. Actually, the determination was more accurate by the self-oscillation spectral analysis. This is true because (1) the forced response was only obtained at a few discrete frequencies and so response peaks were not fully defined, and (2) because the high amplitudes achieved during the pulsing may have introduced shifts of response peaks due to nonlinear behavior. Moreover, some question had been raised about whether the action of the pulser would affect the normal pump inlet cavitation. This might be due to the existence of abnormal mechanical vibration, or to disturbance of flow conditions at the pump inlet (see Fig. 2). The degree of agreement of the pulsing and non-pulsing results dispelled any major concern in this regard.

The oxidizer resonance determined from the pulsing tests is at 7.5 Hz for the pump operating conditions applicable for Fig. 3. In this case the auto-spectrum of oxidizer pressure does display an identifiable oxidizer suction line resonant peak. Frequently, however, a broad low-frequency region of relatively high energy exists, with a number of superimposed minor peaks confusing the assessment. Consistent determination of the oxidizer resonance over a wide range of pump operating conditions has not been possible from analysis of self-oscillation either during ground tests or from flight. Determinations have tended to be more successful for low pressure operation of the pump for which Fig. 3 is an example.

These results typify the ability to detect fuel and oxidizer suction resonant frequencies from static firings on test stands having vehicle configuration suction lines, and when accumulators are not present. For routine evaluation of engine steady performance, it is common practice to static fire engines on stands which possess much longer suction lines than these on the flight vehicle. It is desirable to detect these suction line resonances, and then infer the pump cavitation compliance. Unfortunately, the clear identification of suction resonances on these test stands has not always been

successful, due in part to the comparatively lesser quality of the instrumentation system. Furthermore, the behavior of the long lines tends to make the determination of pump cavitation compliance less accurate.

Prior to flight test of accumulators, static firings are made on test stands having vehicle configuration suction lines. The presence of an accumulator causes a substantial reduction in the first resonant frequency of the suction line -- for that is the accumulator's purpose. The detectability of the reduced frequency has met with mixed success in the Titan experience. Part of the reason seems to be the fact that the accumulator reduces the magnitude of self-induced pressure oscillation. Most likely this is due to the effect of the accumulator in smoothing the flow field at the pump inlet. An example of successful detection is found in Section IV.

## B. VEHICLE FLIGHTS

Among the objectives for the spectral analysis of random data from flight vehicles are

1. Detection of suction line resonances when accumulators are not present to identify any atypical degree of cavitation of the pumps
2. Inference of the performance of accumulators by observing their effect on suction line resonant frequencies
3. Identification of frequencies of longitudinal structural modes of the vehicle for comparison with predictions of the structural dynamic model

It has been relatively easy to identify fuel suction resonant frequencies from low-level self-oscillations in flight data. In one particular flight, during which an instability was observed, this determination for the two Stage I engines revealed the fuel resonance for one engine to be several Hz below nominal. It is postulated that its fuel pump was cavitating excessively for some unknown reason. The incorporation of this abnormally low fuel resonant frequency on one engine led to an improved correlation of the stability analysis with the flight observations in terms of the time of occurrence of the instability.

The accurate detection of oxidizer suction frequencies from flight data has met with limited success. The reasons are of the same nature as previously stated in connection with engine static firings. A gross shift in oxidizer pump cavitation would probably be discernible, although a quantitative evaluation might be difficult.

There was a great deal of success in monitoring the performance of the accumulator devices employed on the Gemini Launch Vehicle. These are shown schematically in Fig. 4. The monitoring was particularly successful for the standpipes located in the oxidizer suction lines. Details of this monitoring effort are presented in Section IV. The piston-type accumulators employed in the fuel suction lines were of concern because of possible sticking or excess friction associated with a sliding seal on the piston. In certain periods of flight the detection of a reduced first resonant frequency was possible, in others it was not. However, at all times a distinctive change in the character of the auto-spectrum of suction pressure indicated that the accumulator was responding to some extent to pressure fluctuations.

The identification of the frequencies of longitudinal structural modes of a flight vehicle has been highly successful. Figure 5 shows a comparison for a particular Titan configuration of analytically-predicted modal frequencies versus time and determinations from accelerometer data during powered flight of Stages I and II. The detection of the frequencies in flight is through auto-spectral analysis of acceleration data. In an effort to maximize the detectability of the modal frequencies, four seconds of data were analyzed with a 1-Hz bandwidth.

Figure 6 is an example of an auto-spectrum at 83 percent of Stage I burn time. The accelerometer which supplied the data for this plot had a range of  $\pm 2.5g$  and was located at the forward end of the launch vehicle. A visual examination of the accelerometer data at this time suggests that a fundamental vehicle frequency can be established by merely counting cycles.

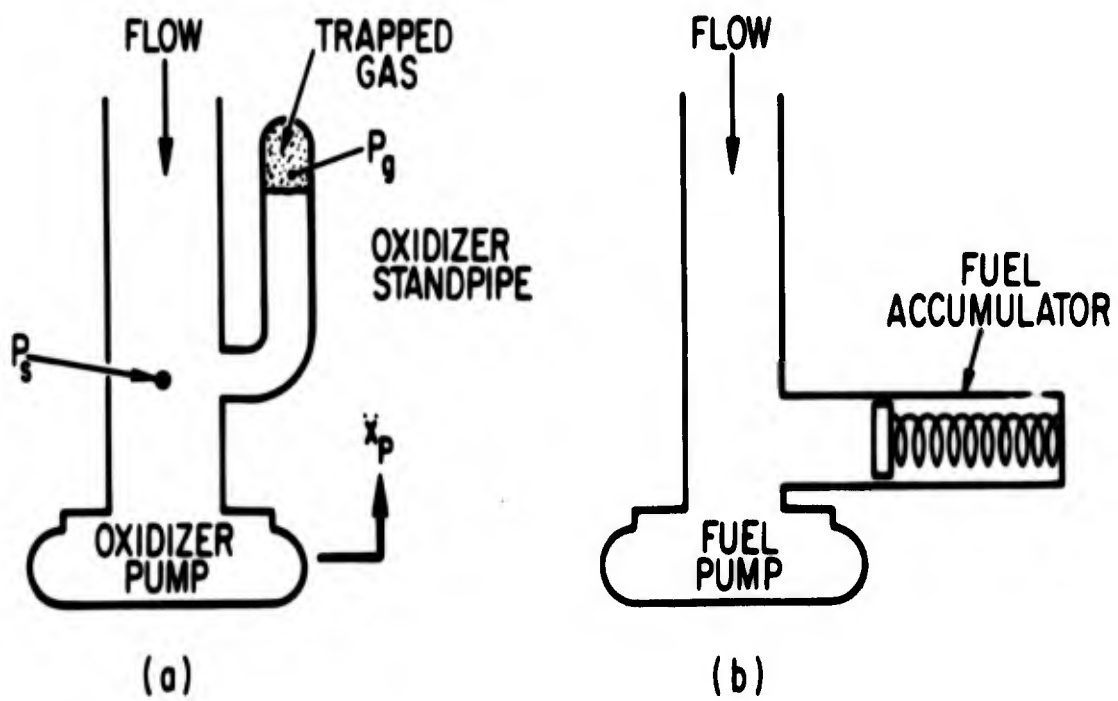


Fig. 4. Schematics of Pogo Accumulators on Gemini Launch Vehicle

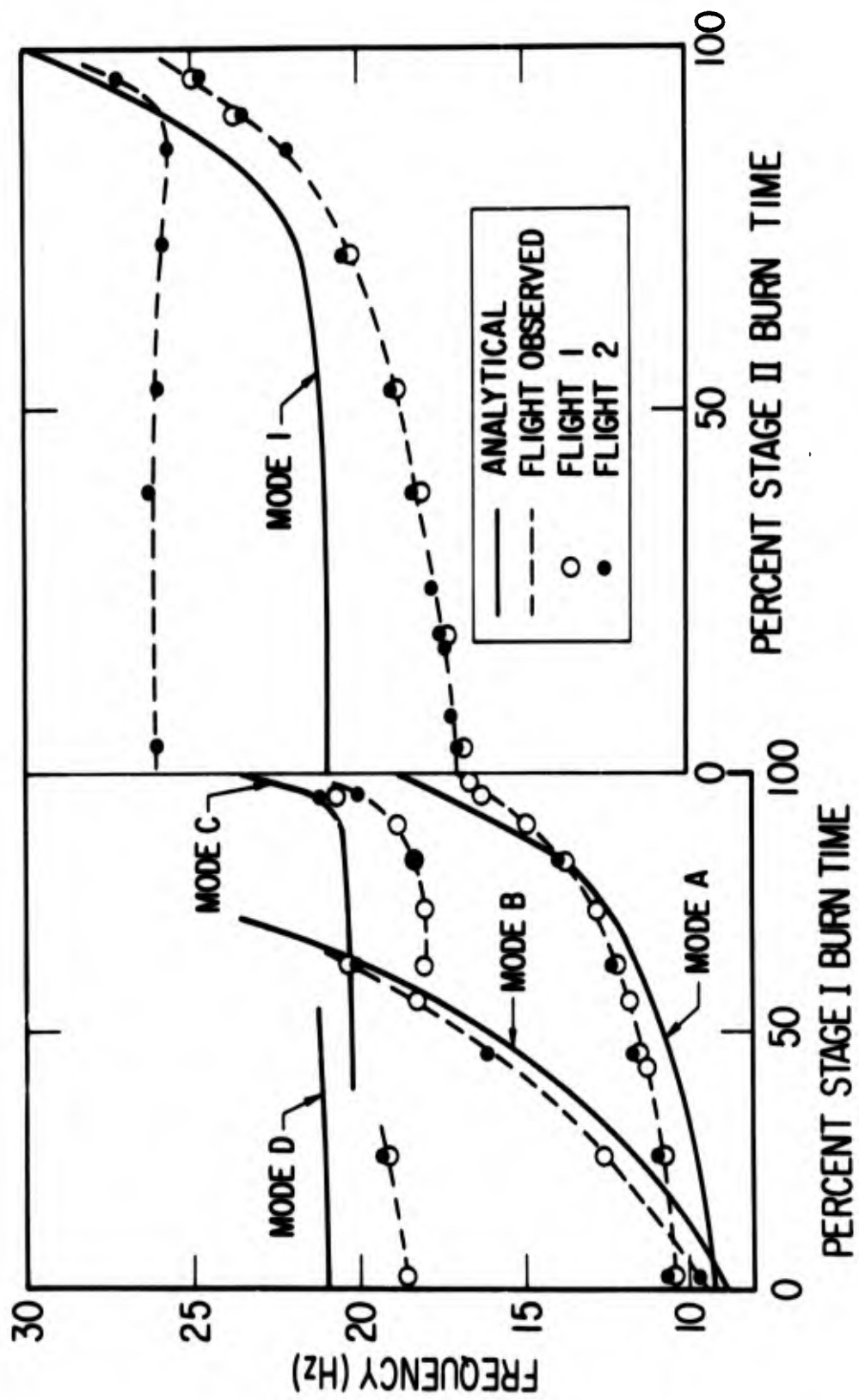


Fig. 5. Analytical Versus Flight-Observed Modal Frequencies

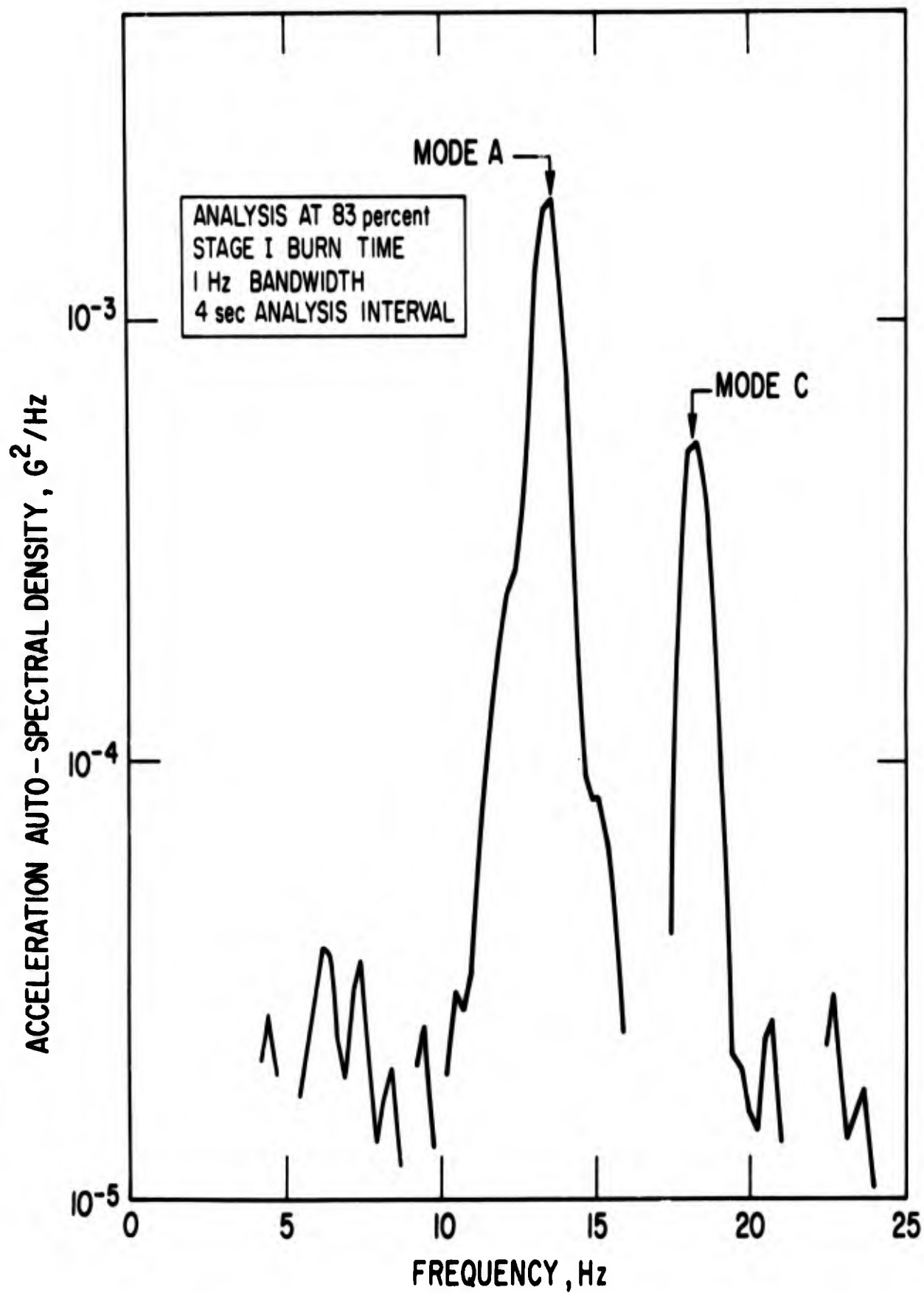


Fig. 6. Auto-Spectrum of Flight Acceleration Data  
(see Fig. 5)

However, experience has shown that the results tend to be erroneous due to the presence of several frequency components. The eye will "detect" a single frequency within the range of 14 to 19 Hz. Moreover, a good deal of scatter will occur for repeated determinations. As can be seen in Fig. 5, at 83 percent of Stage I burn time the two peaks result from the two structural modes A and C.

The lack of agreement between analytically-derived and flight-derived modal frequencies in Fig. 5 led to an investigation of possible errors in the structural dynamic model. A successful effort to pinpoint errors in the model through additional use of the flight data is described in Section V.

**BLANK PAGE**

#### IV. EVALUATION OF A STANDPIPE ACCUMULATOR

In the preceding section interpretation of peaks in spectral density analyses of flight and engine test data led to definition of resonant frequencies. In this and the following section, although use is again made of the character of the frequency content of the data, primary emphasis is on methods of utilizing frequency-response relationships determined from auto- or cross-spectral density analyses of two signals (Ref. 5). The methods rely on the existence of simple input-output relationships among the measured parameters. A determination of frequency-response functions yields specific information on the dynamical characteristics of portions of the structural/propulsion system.

In the following we consider how analysis of random pressure oscillations was used to evaluate the operation and effectiveness of a standpipe accumulator which was installed in the oxidizer suction line of the Gemini/Titan booster. An anomalous occurrence of a Pogo instability on the fifth Gemini/Titan flight (GT-5), directly related to the standpipe operation, makes this a particularly interesting example.

The oxidizer standpipe, shown schematically in Fig. 4, introduces a high volumetric compliance near the pump inlet in the form of a quantity of trapped gas. This "bubble spring," together with the propellant mass in the standpipe, comprise a simple vibration absorber tuned to the frequency  $f_a$ . The effects on the dynamic characteristics of the suction system are indicated by the frequency-response curve of suction pressure per unit acceleration of the pump,  $p_s/\ddot{x}_p$ , as shown in Fig. 7. In the frequency range of interest, the standpipe does the following: (1) lowers the first suction line resonance to  $f_1$ ; (2) introduces an antiresonance at the standpipe tuning frequency  $f_a$ ; and (3) introduces an additional system resonance  $f_2$ . Analysis objectives were simply to verify that these features existed in accordance with predictions of the analytical model.

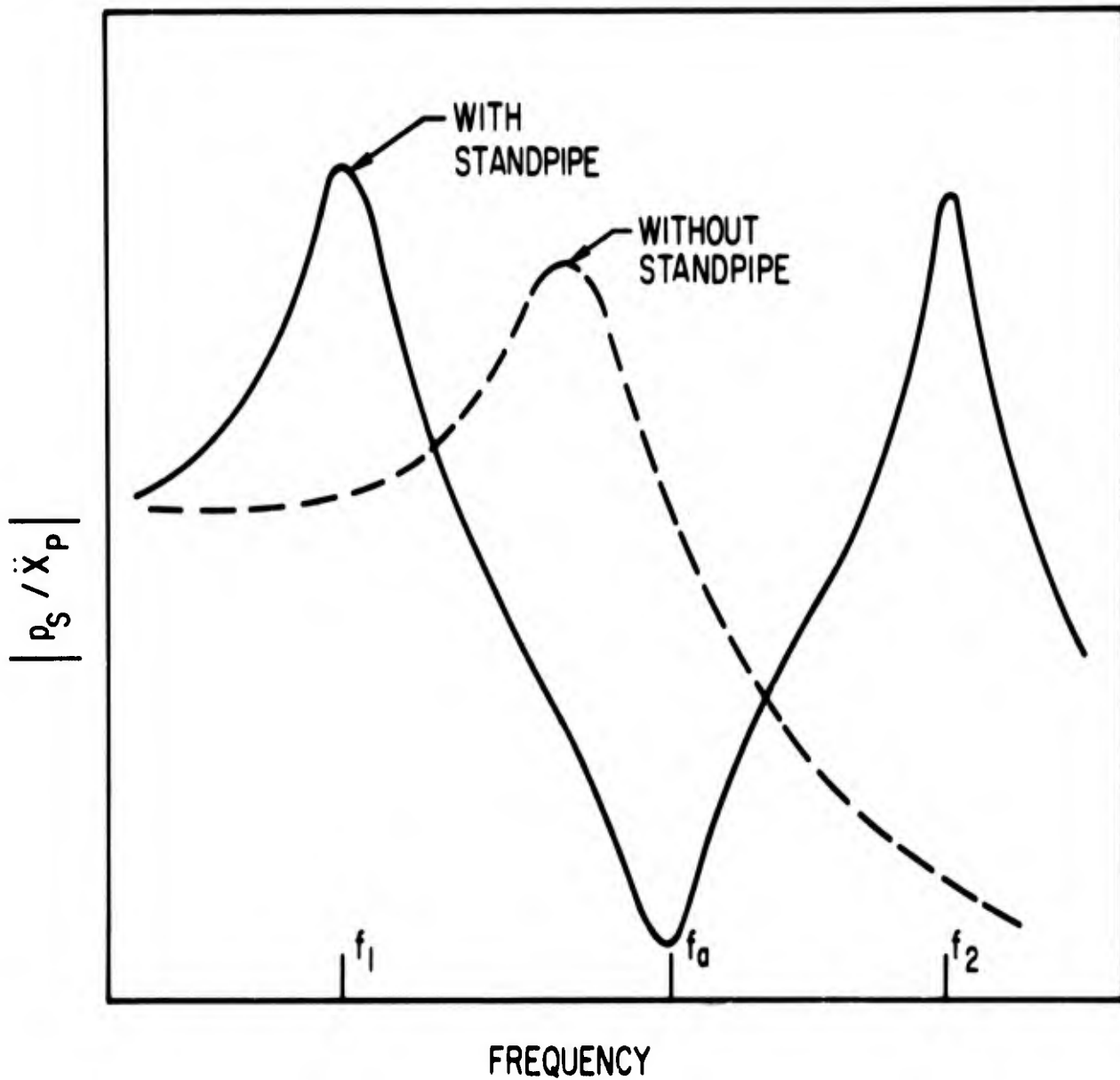


Fig. 7. Effect of Standpipe on Suction Pressure per Unit Pump Acceleration

Pertinent data analyzed were measurements of standpipe gas pressure  $p_g$  and suction pressure  $p_s$  in the oxidizer line. The suction system resonances  $f_1$  and  $f_2$  were determined by inspection of auto-spectral density analyses. The antiresonant or tuning frequency  $f_a$  was best identified from the characteristics of the ratio  $p_s/p_g$  which was determined from the data by means of cross-spectral density analyses. If we neglect minor structural acceleration effects, this frequency-response function is a simple antiresonant characteristic (inverse of a single degree of freedom resonant characteristic) exhibiting an amplitude minimum and a rapid phase shift through 90 degrees at the frequency  $f_a$ .

Figure 8 shows one of the better examples of an auto-spectral analysis of oxidizer suction pressure. The first and second suction line resonances are clearly evident. Although a general peaking of the auto-spectrum always occurred in the expected region of the second resonance, in some cases this resonance was not so clearly defined as in this example. The spectrum also gives an indication of a minimum in the expected region of the standpipe tuning frequency. Indeed, the striking similarity between the auto-spectrum of Fig. 8 and the theoretical function of Fig. 7 should be noted.

To define the tuning frequency more quantitatively, the frequency-response function for  $p_s/p_g$  was determined from the data, as exemplified in Fig. 9. The following three items were jointly considered in arriving at a specific value for the tuning frequency: (1) the frequency of an actual minimum in the amplitude ratio; (2) the frequency of minimum amplitude ratio implied by trends in the data away from the "dip" region, and (3) the frequency of 90 degrees phase shift. The effects of uncertainties in the data because of low amplitude response in the region of the tuning frequency were thus minimized. It was frequently found that the rapid phase shift through 90 degrees, indicative of light damping, made the phase data a particularly good indicator of the tuning frequency. For the example a frequency of 14.2 Hz was deduced from the data. Regions of excellent data coherence ( $>0.95$ ) are also indicated in Fig. 9; such coherence was always found near

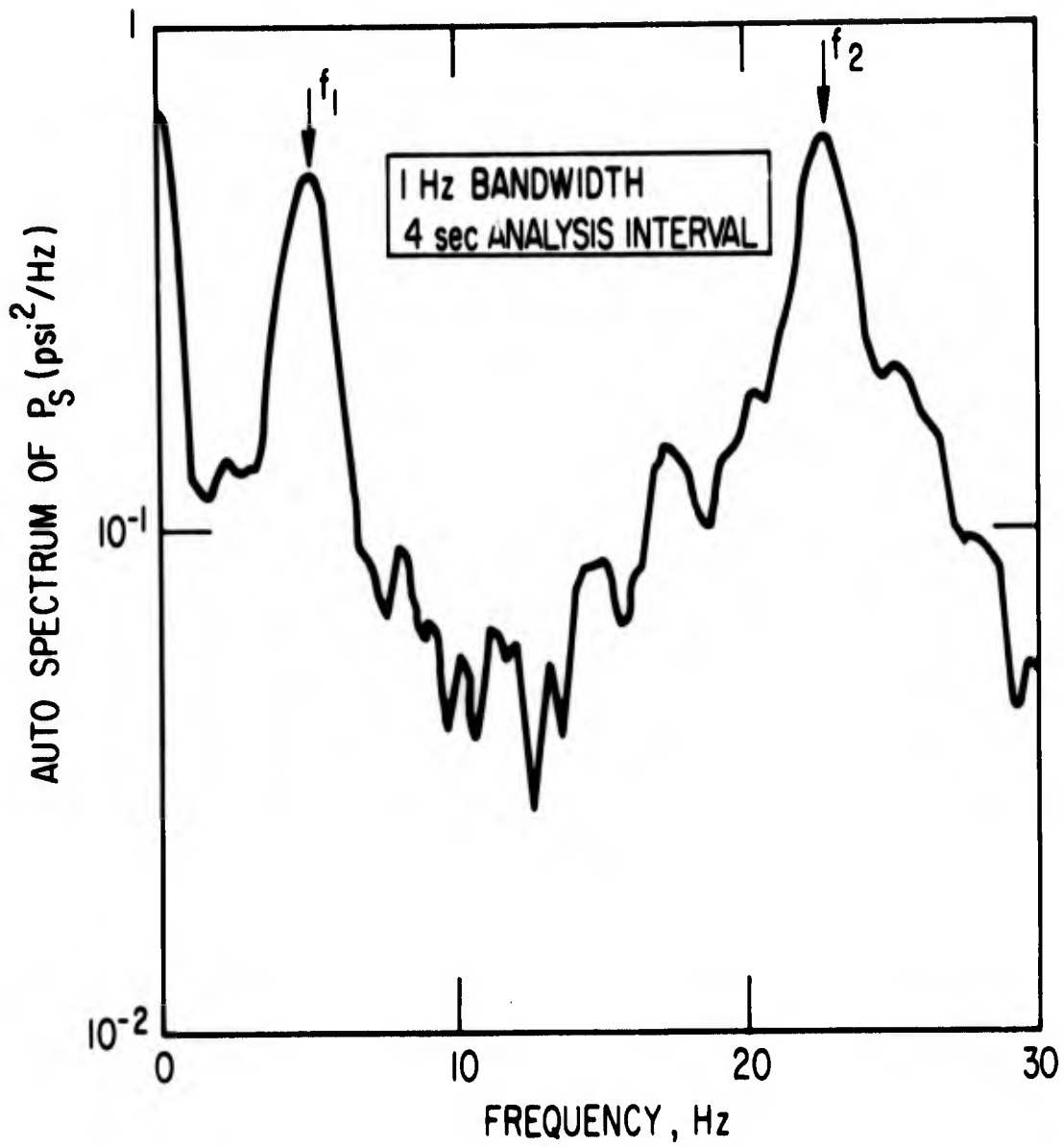


Fig. 8. Auto Spectrum of Oxidizer Suction Pressure with Standpipe From GT-4 at 60 Percent Stage I Burn Time

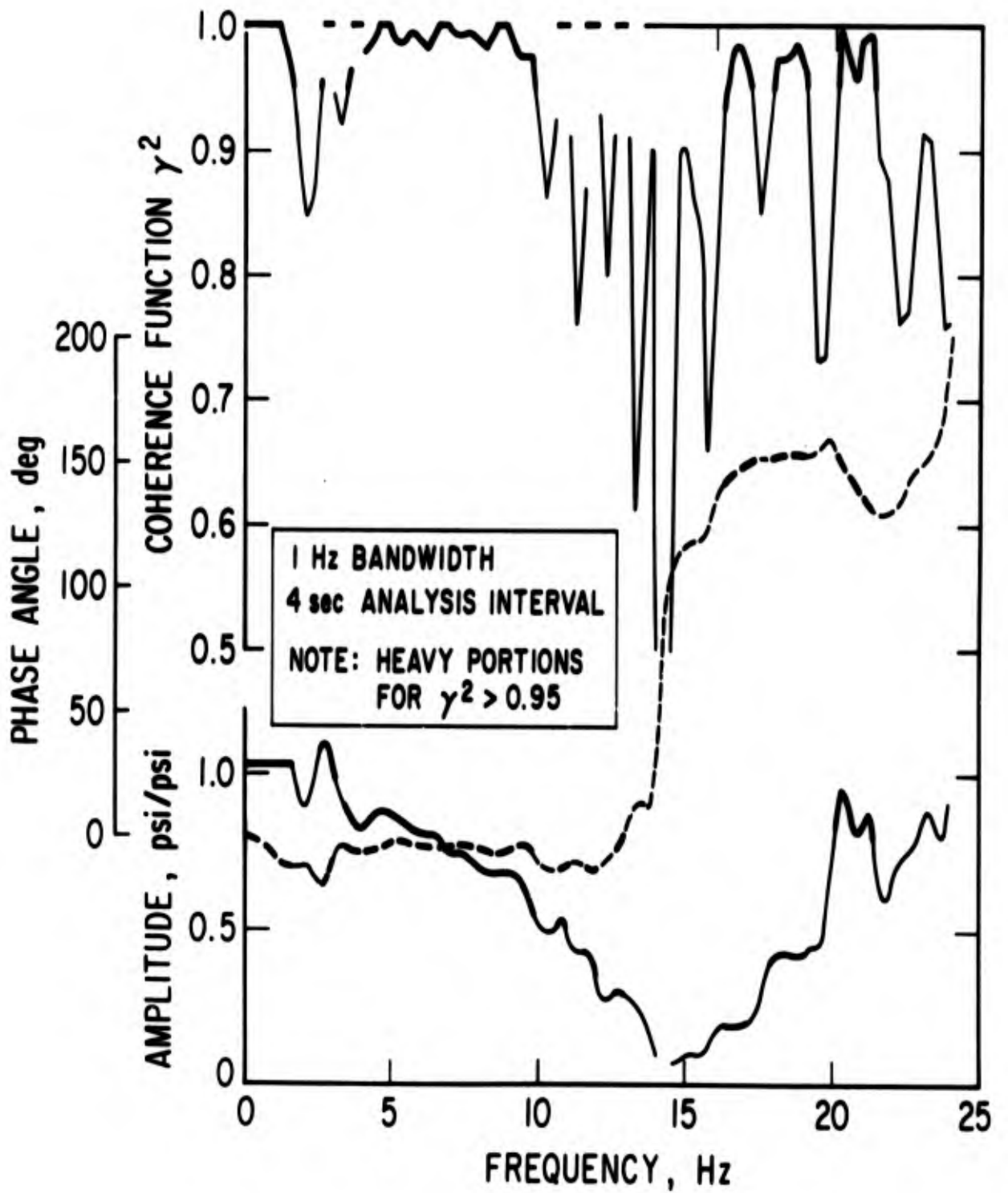


Fig. 9. Frequency Response  $p_s/p_g$  and Coherence Function from GT-4 Flight at 97 Percent Burn Time

the lower resonant peak  $f_1$ . Although reasonably good coherence (above 0.8) was found in off-resonance portions of the data, coherence in the immediate vicinity of the tuning frequency was poor.

The immediate benefit of the flight data analysis was verification that the standpipe operation was satisfactory. By repeating the analysis procedure at a sequence of flight times, it was determined, however, that for some flights as much as 36 percent of the trapped gas was gradually lost, probably through absorption. Although the amount was significant, analytical studies indicated that the observed gas loss was not detrimental for Pogo stability.

One of the most important benefits of the data analysis became evident after the occurrence of an instability on GT-5. By the use of results of stability analyses and data analyses from the first four flights as a reference, spectral analyses of random data just after vehicle liftoff showed quickly and conclusively that the anomaly was the result of an insufficient gas charge within the standpipes. This identification of the deficiency led directly to correction of an improper preflight charging procedure newly introduced for the fifth flight.

Since the standpipe tuning frequency is directly related to the gas volume, it is the ratio  $p_s/p_g$  which provides the clearest evidence of an inadequate charge. Figure 10 is a comparison of data just after liftoff for GT-5 and GT-4, the latter being representative of a normal flight. The standpipe frequency for GT-5 was 25 Hz compared to 7.8 Hz for GT-4, indicating a gas charge of less than 10 percent of nominal at this time.

The anomalous nature of the GT-5 oxidizer suction system is also clearly indicated in the auto-spectral density plots of Fig. 11. Although the information is less quantitative, the obvious upward shift in both the first suction line resonance and the characteristic "dip" in the spectrum (usually seen at about 8 Hz) indicates very low gas charge. A feature of this figure is

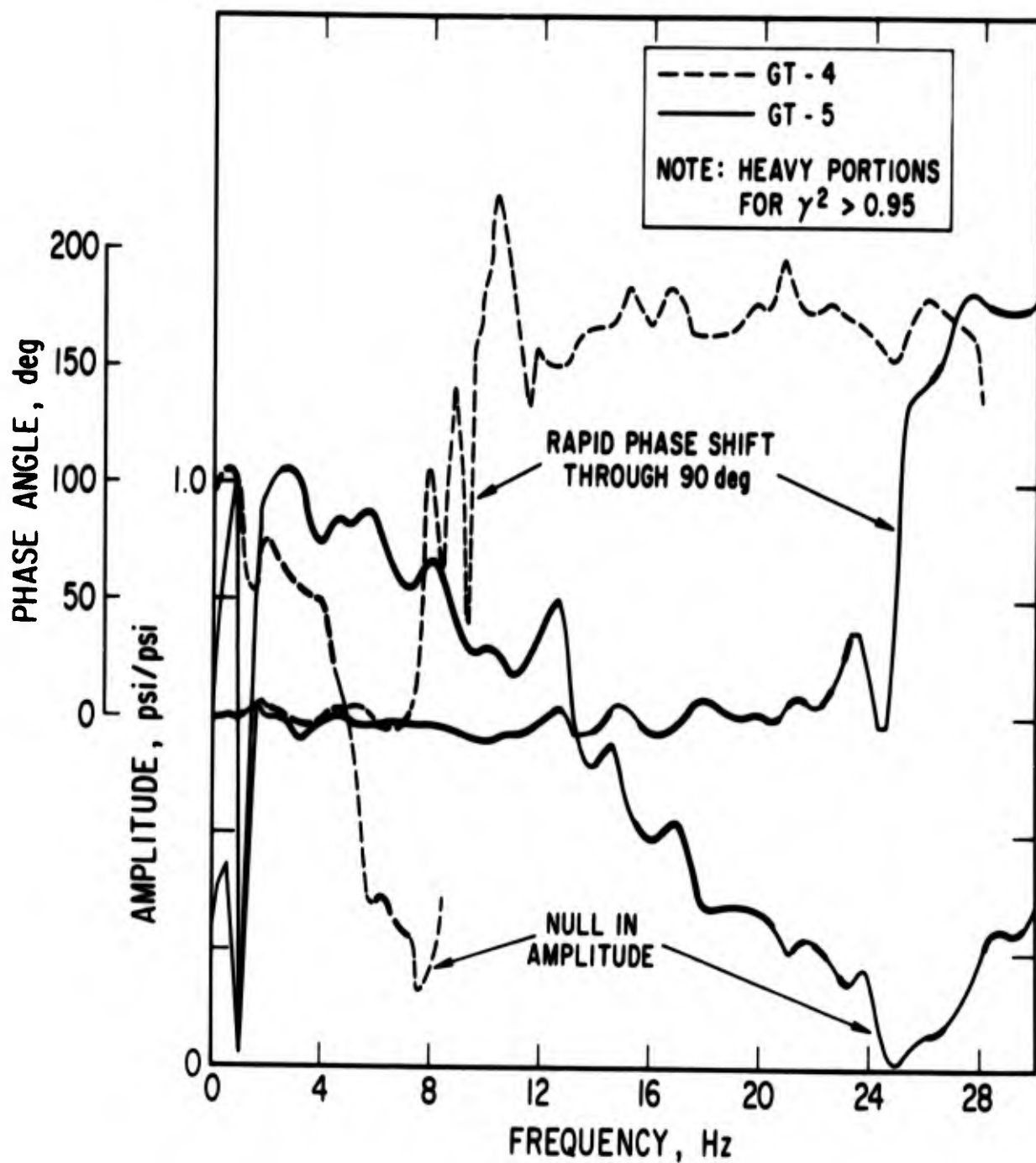


Fig. 10. Frequency Response  $p_s/p_g$  from GT-4 and GT-5 Flights at 2.5 Percent Stage I Burn Time

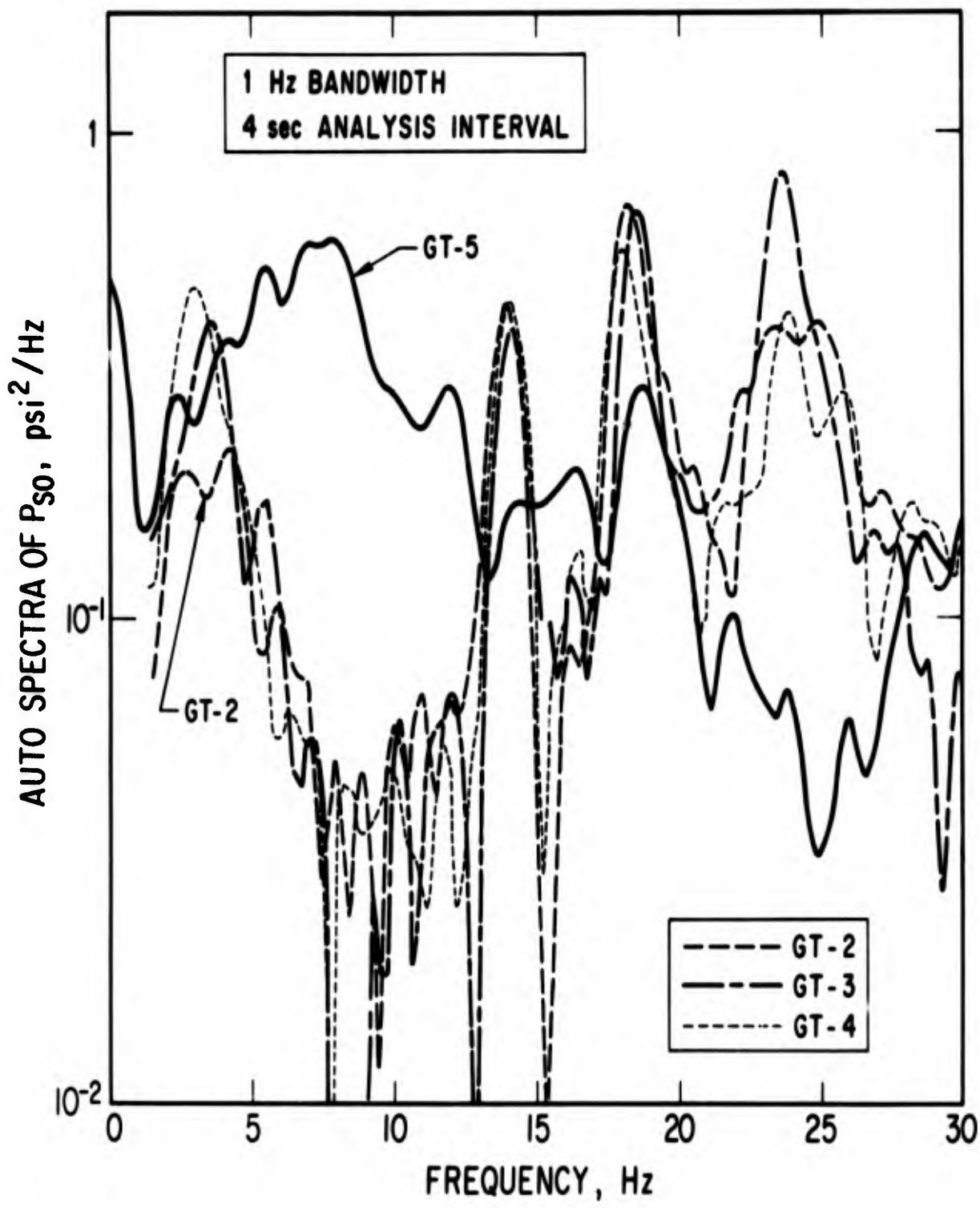


Fig. 11. Auto Spectra of Oxidizer Suction Pressure  $p_{s0}$  for Several Flights

the repeatability of the data from flight to flight. Its significance lies not only in the evidence of the GT-5 anomaly but also in the fact that GT-2 would be classed normal, even though a characteristic first suction line resonance could not be definitely determined. The consistency of this data leads one to conclude that the use of auto-spectral analyses to establish norms for flight data can be a valuable tool in detecting and interpreting anomalous behavior.

**BLANK PAGE**

## V. EVALUATION OF THE LONGITUDINAL STRUCTURAL DYNAMIC MODEL

Stringent accuracy requirements on the description of significant longitudinal structural modes for Pogo stability analyses have provided a strong incentive for evaluating the vehicle dynamic model. Moreover, the increasing complexity of space systems tends to require greater modeling accuracy for such studies as the determination of structural dynamic loads resulting from propulsive transients. We will now briefly describe a novel technique for utilizing low-level random flight accelerometer data to evaluate the longitudinal dynamic model of the vehicle. The practicality of the method is indicated by presentation of a particular result of its application.

For a given accelerometer, we imagine that the vehicle is divided into two parts. One part consists of the vehicle section forward of the accelerometer station, and the other part is the remaining aft vehicle section. The new approach seeks to determine from flight data one or more natural frequencies for these forward and aft sections, assuming each is "base-fixed" at the accelerometer station. Comparison of the flight-derived natural frequencies with corresponding frequencies determined from the dynamic model permits an independent assessment of modeling accuracy for each vehicle section. A degree of localization of inaccuracies in the over-all vehicle model is achieved by performing this determination for several accelerometer locations and logically combining the results.

The basics for this concept are shown schematically in Fig. 12 for two accelerometers at locations designated "a" and "b". Ideally, analysis of the data from these two accelerometers would lead to definition of natural frequencies for vehicle sections I-II and III in Fig. 12b, and sections I and II-III in Fig. 12c. In this case it would be possible to detect existence of modeling deficiencies in each of the sections I, II, and III.

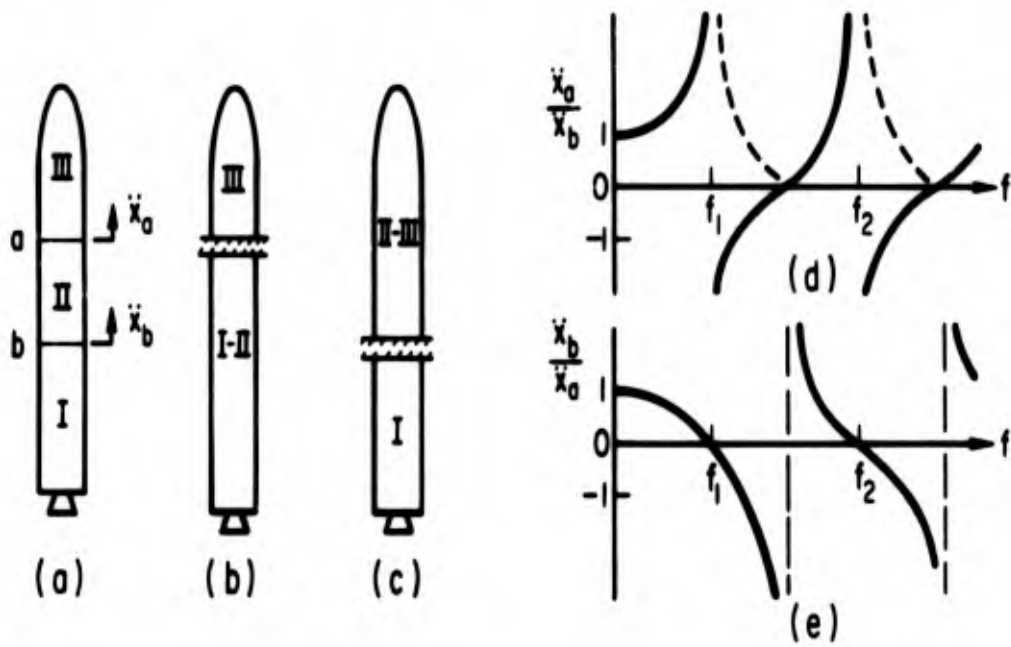


Fig. 12. Basics for "Node-Frequency" Detection

A base-fixed natural frequency is one for which a longitudinal node must exist at the base position when vehicle oscillations occur at this frequency. Such a "node frequency" is of special significance when it also corresponds to the frequency of a free vibrational mode of the vehicle. Since the node represents a lack of longitudinal vibrations, the imposition of a fixed longitudinal constraint at this point in no way affects the vehicle vibration in that mode. Accordingly, this "node frequency" corresponds to a natural frequency for both the forward and aft sections of the vehicle when each is base-fixed at the node position. If, however, a "node frequency" is not equal to that of a free vibrational mode of the over-all vehicle, this "node frequency" as we shall see is only meaningful for one of the vehicle sections.

The usefulness of this approach clearly depends on devising an accurate technique for using the flight data to determine the "node frequencies" associated with each accelerometer. Consider the problem of defining a "node frequency" for position "b" in Fig. 12a. If no external forces exist forward of position "b", then the response throughout section II-III is completely determined by the base motion  $\ddot{x}_b$ . Let  $\ddot{x}_a$  denote a particular measured acceleration response. The ratio  $\ddot{x}_a/\ddot{x}_b$ , as a function of frequency, has the form shown in Fig. 12d for an undamped system. Positive ratios denote "in-phase" motion; negative ratios denote "out-of-phase" motion. The magnitude of the frequency response (shown as a dashed line when the response is out-of-phase) indicates familiar resonant behavior (that is,  $|\ddot{x}_a/\ddot{x}_b| \rightarrow \infty$ ) at frequencies  $f_1, f_2, \dots$ , corresponding to the fixed-base natural frequencies for the section II-III. The "inverse frequency-response" function  $\ddot{x}_b/\ddot{x}_a$  will exhibit the characteristics shown in Fig. 12e, where the frequencies  $f_1, f_2, \dots$ , manifest themselves as frequencies of zero base motion (that is, as "node frequencies" for position "b").

The scheme to determine a "node frequency" for position "b" is based on using random data to establish a zero crossing of the ratio  $\ddot{x}_b/\ddot{x}_a$ . In practice values of the ratio at discrete frequencies are obtained on one or

both sides of a zero crossing. A zero crossing ("node frequency") estimate is then obtained by extrapolation or interpolation. Reliance on inaccurate data immediately adjacent to the "node frequency" is avoided.

For the case of the standpipe, spectral analyses allowed the determination of frequency response over a wide range of frequencies because of high coherence in that range. However, the acceleration data were found to be coherent only within narrow frequency bands centered on the modal frequencies of the over-all vehicle. Thus, in a given time interval, it was only possible to determine a valid amplitude ratio at a modal frequency. However, since the vehicle natural frequencies vary with time due to propellant depletion, ratios are obtained for a series of frequencies by analysis at a sequence of times. It was found that the coherence was quite high at the structural frequencies, so that equally accurate ratio magnitudes could be obtained from cross-spectral or auto-spectral analyses (see Eq. (2)). The cross spectra, however, also establish the phasing.

The present technique permits the use of data from several vehicle modes, from many times of flight, and even from different stages of flight to accurately determine "node frequencies". It requires a minimum of data accuracy; uncalibrated instruments can yield identical results if they are "reasonably well behaved" in the frequency range of interest. Also, the results lead to a useful quantitative evaluation of the model accuracy. Finally, by the nature of the technique, the use of only a few longitudinal accelerometers leads to a relatively high degree of localization of areas where modeling inadequacies exist. The present technique has distinct advantages for checking the dynamic model over "traditional" efforts involving determination of mode shape.

#### A. DETECTION OF MODELING DEFICIENCIES

The preceding method was applied to data obtained from the Titan vehicle configuration shown in Fig. 13. A lack of satisfactory correlation between analytically-derived and model-derived modal frequencies during the latter portion of Stage I burn and during Stage II burn, as shown in Fig. 5,

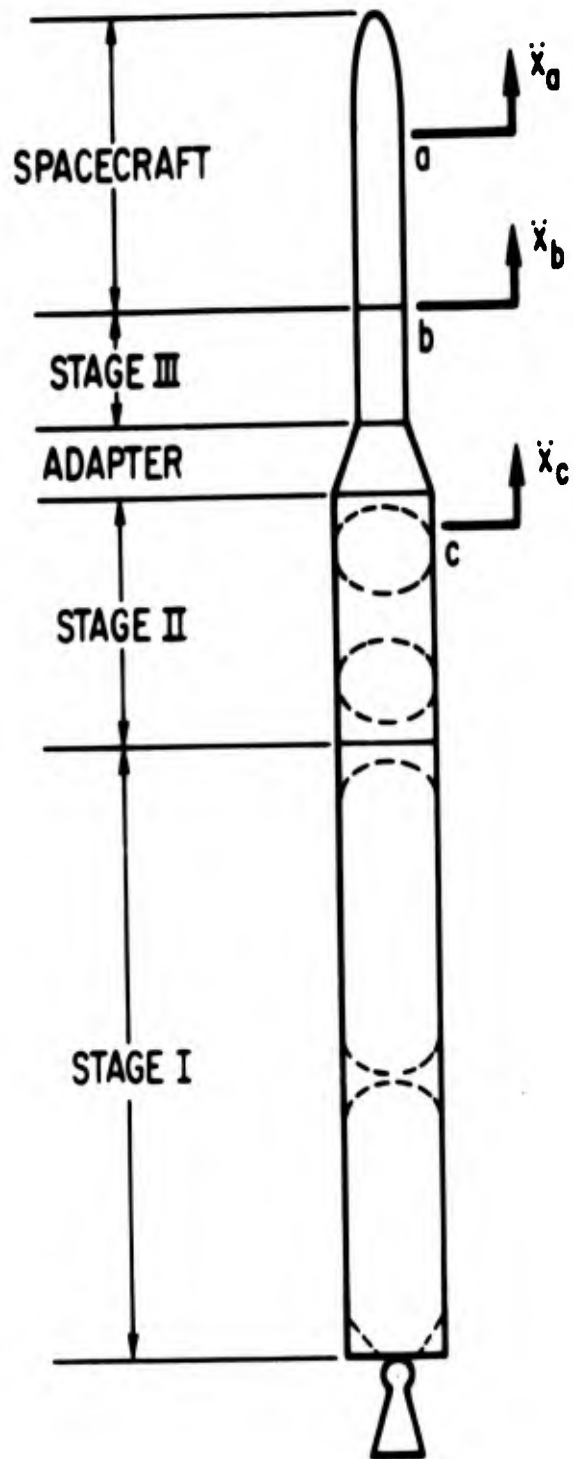


Fig. 13. A Titan Vehicle Configuration

prompted an attempt to seek modeling deficiencies. In an initial analysis "node frequencies" were determined for the two positions "b" and "c" in Fig. 13. Position "c" was just forward of the Stage II propellant tanks; position "b", at the base of the spacecraft. Position "a" within the spacecraft was used to determine a "node frequency" for position "b".

The accelerometers employed had a range of  $\pm 1$  g and measured oscillatory accelerations only. The rms values of the accelerations in the vehicle modes were less than 0.05 g; hence, the narrow-range of these accelerometers was essential to the quality of the results.

Ratio points leading to estimates of the zero crossings in the ratios  $\ddot{x}_c/\ddot{x}_b$  and  $\ddot{x}_b/\ddot{x}_a$  are shown in Fig. 14. The open points are derived from observations of the two structural modes A and C (see Fig. 4) of the over-all vehicle during Stage I burn; the closed points, from the lowest mode during Stage II burn. The curves indicate a "node frequency" of 16.5 Hz for position "c" and 26.0 Hz for position "b".

For the forward vehicle section base-fixed at position "c", the analytical model yielded a first natural frequency of 19.5 Hz, compared with the flight-derived value of 16.5 Hz. The conclusion, assuming proper mass modeling, is that the over-all model stiffness forward of station "c" is too high. The model for the vehicle section aft of position "c" yielded a natural frequency of 16.3 Hz compared to the observed 16.5 Hz; this was considered to be satisfactory agreement. The spacecraft model, base-fixed at position "b", yielded a first resonant frequency of 23.9 Hz, compared with the observed frequency of 26.0 Hz. This implies that the spacecraft model stiffness was too low. This, coupled with the conclusion that the model stiffness forward of position "c" was too high, leads to the conclusion that an overly high model stiffness exists for the vehicle section between positions "b" and "c". On the basis of other information the most probable explanation was an overly high stiffness of the adapter section. This was subsequently verified when the same method of analysis was applied to accelerometer data from locations along the forward skirt of Stage II and the adapter. The final conclusion was that the actual stiffness of the adapter was only about 40 percent of the original model value.

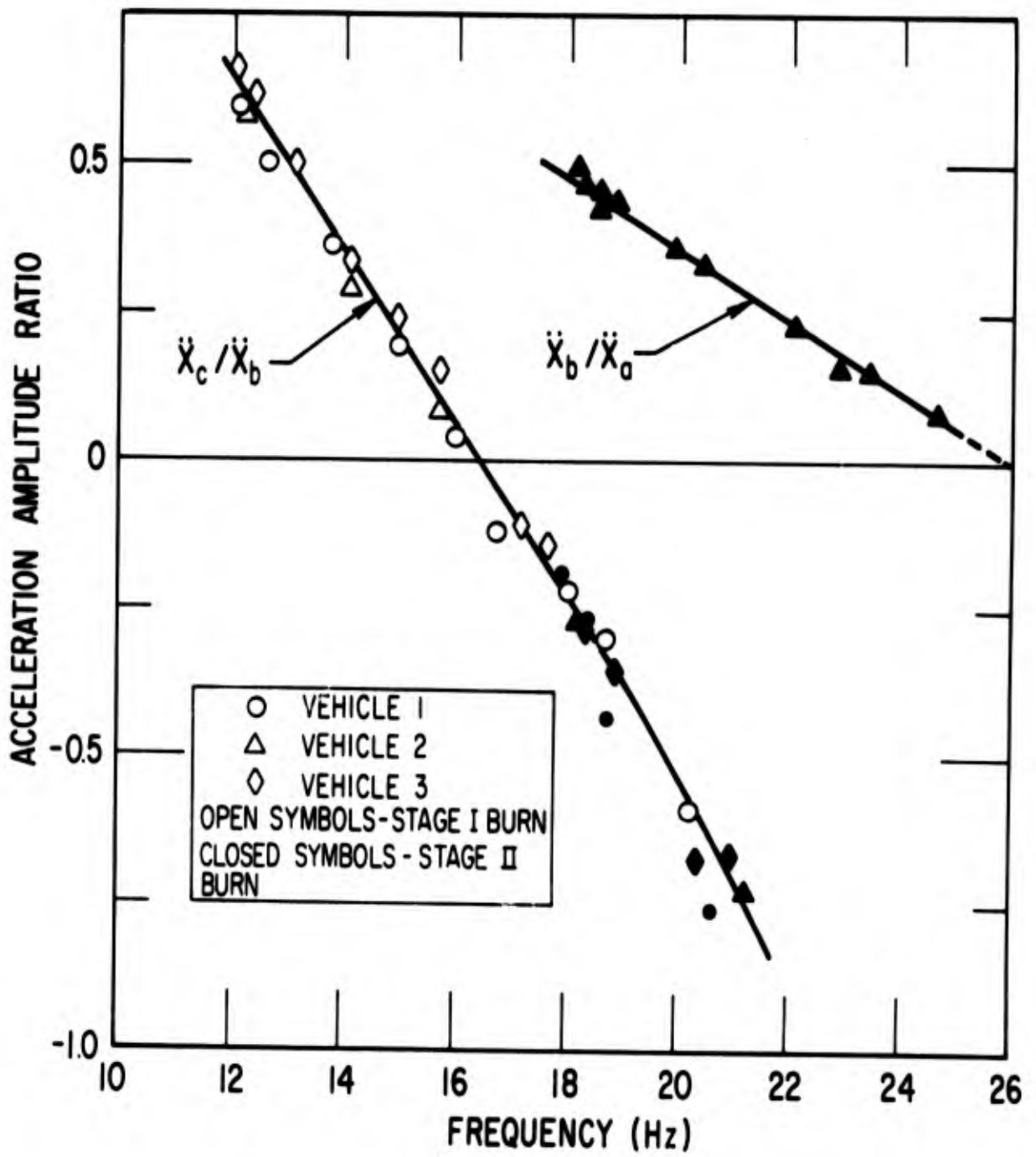


Fig. 14. Acceleration Amplitude Ratios Versus Frequency

Figure 15 shows the flight-observed natural frequency curves during Stage II burn, and the single frequency curve from the original model (the only one below 30 Hz); these curves appear also on Fig. 5. Two degrees of improvement in the accuracy of the first two natural frequencies are also shown in Fig. 15. One change introduces a revised adapter stiffness only, and produces a major improvement in the correlation with the flight-derived frequencies. The second change introduces, as well, an increase in spacecraft stiffness to raise the calculated spacecraft base-fixed frequency for better agreement with the flight-derived value of 26.0 Hz. The additional improvement in correlation is evident.

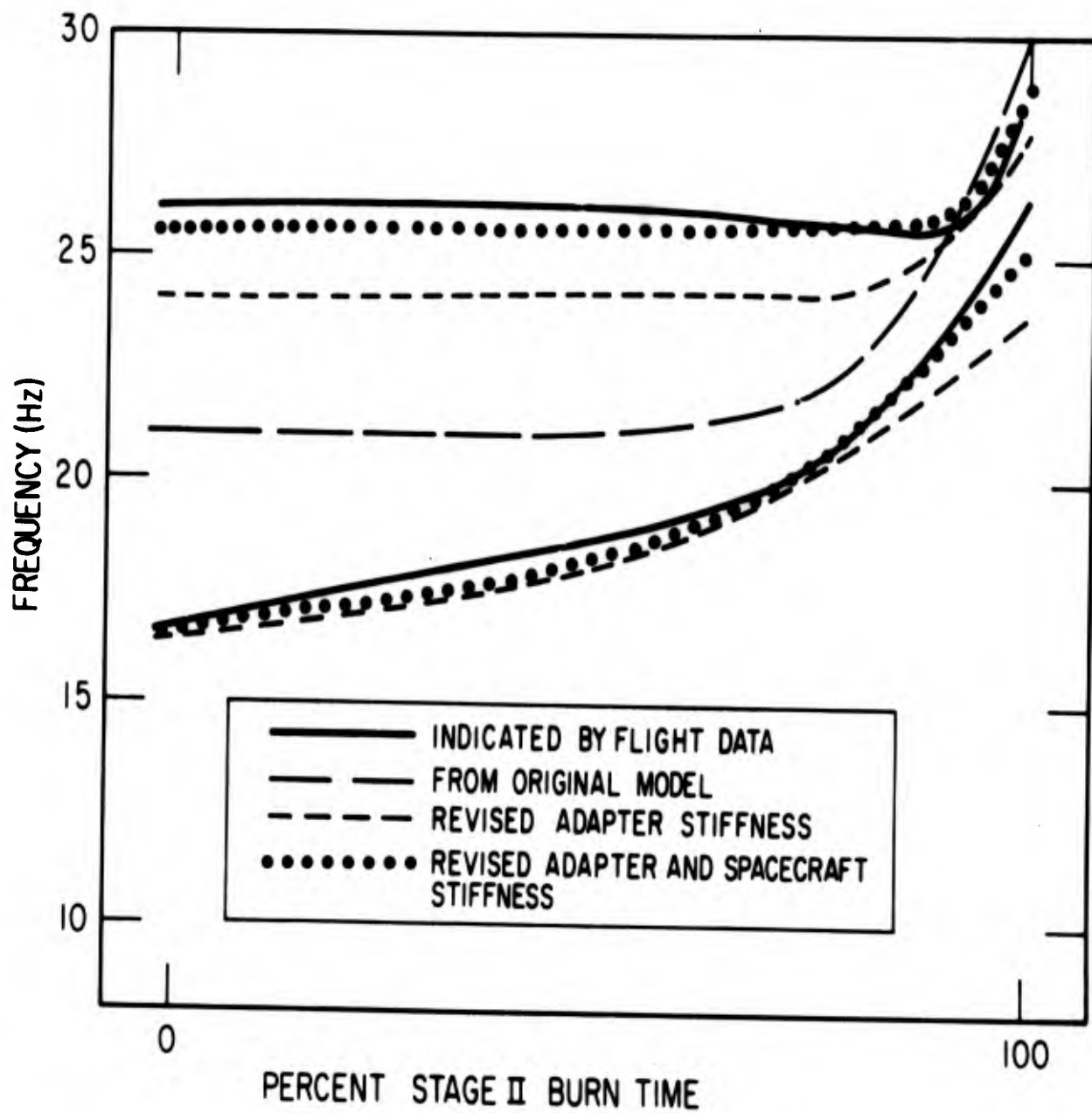


Fig. 15. Analytical Versus Flight Observed Modal Frequencies, Stage II Burn

## VI. SUMMARY AND CONCLUSIONS

The Pogo phenomenon is the result of an instability arising from a dynamic coupling of the structural and propulsion systems of a space vehicle during boost flight. The strong oscillations observed during an instability are a display of the mode of that instability. This mode is so dominant that it effectively masks broader aspects of the system behavior.

During stable flight and during engine static firings, low-level random oscillations occur as a result of broad-band random excitations. The oscillations contain frequency-response information for the system. Even though this "system noise" generally lies within a few percent of the range of the measurement system, much quantitative knowledge of system characteristics has been extracted.

The knowledge was derived from auto-spectral and cross-spectral density analyses of the random data. Much of the analysis was characterized by eight statistical degrees of freedom; for example, a 1-Hz analysis bandwidth with a four-second data sample. Short analysis times were dictated by a desire to restrict smearing of the system properties resulting from variations of those properties with time; the use of relatively narrow bandwidths arose from a desire to discriminate between adjacent concentrations of energy in the spectral results. Good engineering results were achieved in locating resonant frequencies, especially those for the lightly-damped structure. Further, valuable frequency-response information was obtained for conditions of high coherence. The presence of high coherence reduces the number of degrees of freedom required for obtaining this information with good statistical accuracy.

Suction line resonant frequencies were detected both in flight and during engine static firings. Better definition of the resonant frequency of the fuel line was obtained by analysis of "self-noise" in the system than resulted from forced sinusoidal oscillation during static firings. The detection of

line resonant frequencies and the determination of frequency-response information during flights of the Gemini Launch Vehicle permitted evaluation of the effectiveness of hydraulic accumulators. In particular, the computation of a pressure frequency-response function for the oxidizer standpipe permitted an accurate detection of its "tuning frequency". This clearly identified the reason for an anomalous occurrence of an instability on a Gemini flight as being the result of inadequate gas charge of the standpipes.

Considerable success has been achieved in detecting resonant frequencies of longitudinal structural modes of the vehicle throughout boost flight. Peaks in auto spectra of low-level random acceleration data identify the modal frequencies quite clearly because of very light damping. Additional knowledge about the longitudinal structural dynamics of the vehicle was gained by using acceleration frequency-response information to identify the frequency at which a longitudinal node would exist at vehicle stations at which accelerometers were located. The method depends on high coherency at vehicle modal frequencies to permit the determination of a ratio of amplitudes at two stations. The ratio is determined for a sequence of flight intervals to make use of changing modal frequencies to define the variation of the ratio with frequency. An indicated zero in the ratio identifies the vehicle natural frequency at which a node would exist at the station used for the numerator. This "node frequency" is then the base-fixed resonant frequency of the vehicle forward of that station, as well as that for the vehicle aft of that station, when the frequency is equal to the frequency of a free vibrational mode of the vehicle.

Data from a few well-placed accelerometers during different stages of vehicle boost flight were employed to define the "node frequency" at several stations for a particular Titan configuration. By this method specific modeling deficiencies were identified. This method is quite practical because (1) only a few accelerometers are required to provide explicit checks on the structural dynamic model, (2) the magnitude of the data need not be accurately known, and (3) inadequacies of the analytical model can be localized.

On the basis of the results presented here, it is concluded that the low-level system response observed during static firings of engines and vehicle flights are a source of valuable information. Consideration should be given to the use of special low-range instrumentation to improve the detection of this low-level random response for analysis of system dynamic characteristics. Observed flight-to-flight consistency of the data indicates that special data need only be obtained on an initial few flights of a system. The acquisition and analysis of random data is particularly justifiable for evaluation of a booster which will see widespread use.

## REFERENCES

1. Rubin, S., "Longitudinal Instability of Liquid Rockets Due to Propulsion Feedback (POGO)," Journal of Spacecraft and Rockets, 3(8), 1966, p. 1188.
2. McKenna, K. J., J. H. Walker, and R. A. Winje, "Engine-Airframe Coupling in Liquid Rocket Systems," Journal of Spacecraft and Rockets, 2(2), 1965, pp. 254-256.
3. Davis, W. F., T. L. Lynch, and T. R. Murray, "Thor 20 Cycle Longitudinal Oscillation Study," Shock and Vibration Bulletin No. 34 (AD-460000), Part 2, Dec. 1964, pp. 177-196.
4. Rich, R. L., "Saturn V Pogo and a Solution," Proceedings of AIAA Structural Dynamics and Aeroelasticity Specialist Conference and the ASME/AIAA 10th Structures, Structural Dynamics, and Materials Conference, Volume on Structural Dynamics, New Orleans, April 1969, pp. 32-41.
5. Bendat, J. S., and A. G. Piersol, Measurement and Analysis of Random Data, John Wiley and Sons, New York, 1966, pp. 98-105, 200-213.
6. "Investigation of the Transfer of Oscillations through the YLR 87-AJ-5 Engine Systems," Aerojet General Corporation, Report BSD TR 65-54, March 1965.

DOCUMENT CONTROL DATA - R&D		
<i>(Security classification of title, body of abstract and indexing annotation must be entered when the overall report is classified)</i>		
1. ORIGINATING ACTIVITY (Corporate author) THE AEROSPACE CORPORATION El Segundo, California		2a. REPORT SECURITY CLASSIFICATION UNCLASSIFIED
		2b. GROUP
3. REPORT TITLE DETECTION OF TITAN POGO CHARACTERISTICS BY ANALYSIS OF RANDOM DATA		
4. DESCRIPTIVE NOTES (Type of report and inclusive dates)		
5. AUTHOR(S) (Last name, first name, initial) R. G. Wagner and S. Rubin		
6. REPORT DATE 69 SEPT 05 74 Feb 81	7a. TOTAL NO. OF PAGES 45	7b. NO. OF REFS 6
8a. CONTRACT OR GRANT NO. F04701-69-C-0066	8b. ORIGINATOR'S REPORT NUMBER(S) TR-0066(5305)-3	
b. PROJECT NO.	8c. OTHER REPORT NO(S) (Any other numbers that may be assigned this report) SAMSO-TR-70-22	
c.		
d.		
10. AVAILABILITY/LIMITATION NOTICES This document has been approved for public release and sale; its distribution is unlimited.		
11. SUPPLEMENTARY NOTES	12. SPONSORING MILITARY ACTIVITY Space and Missile Systems Organization Air Force Systems Command Los Angeles, California	
13. ABSTRACT <p>Dynamic characteristics of Titan vehicles related to the Pogo phenomenon have been found through the analysis of low-level random accelerations and pressures from ground test and flight data. Natural frequencies of vibration of propellant suction lines and of flight vehicle longitudinal motion have been successfully detected from locations of peaks in auto spectra. The inflight performance of a standpipe accumulator has been evaluated by means of both auto-spectral and cross-spectral analyses. An anomalous occurrence of Pogo vibration on one flight was explained by the analysis as due to a lack of normal gas charge in the standpipes. A novel method is applied to the evaluation of the longitudinal structural dynamic model of the vehicle. The method involves the detection of "node frequencies" at locations of accelerometers. By this method specific modeling deficiencies were identified and corrected for a Titan vehicle configuration, thereby greatly improving the correlation of flight-derived and analytical natural frequencies.</p>		

Page instability  
Detecting system dynamic characteristics  
Random vibration data  
Spectral analysis  
Booster vehicles  
Engine static firings  
Flight tests  
Longitudinal structural dynamics  
Propellant line dynamics  
Pump cavitation compliance  
Hydraulic accumulators

Abstract (Continued)